Catalytic properties of zirconocene-based systems in 1-hexene oligomerization and structure of metal hydride reaction centers

Lyudmila V. Parfenova,*[,a] Pavel V. Kovyazin,[a] Almira Kh. Bikmeeva,[a] Eldar R. Palatov,[a] Pavel V. Ivchenko,[b,c] Ilya E. Nifant'ev,[b, c] Leonard M. Khalilov[a]

[a] *Institute of Petrochemistry and Catalysis, Ufa Federal Research Center, Russian Academy of Sciences, 450075 Ufa, prosp. Oktyabrya, 141, Russian Federation*
[b]*Department of Chemistry, Lomonosov Moscow State University, 119991 Moscow, 1-3 Leninskiye Gory, Russian Federation*
[c]*A.V. Topchiev Institute of Petrochemical Synthesis, Russian Academy of Sciences, Leninsky prosp. 29, 119991 Moscow, Russian Federation*

Supporting Information

Figure S1. ^{1}H and ^{13}C NMR of 1-hexene oligomers obtained in the system *rac*-$Me_2CInd_2ZrCl_2$ (**1g**) − $HAlBu^{i}_2$ − $(Ph_3C)[B(C_6F_5)_4]$

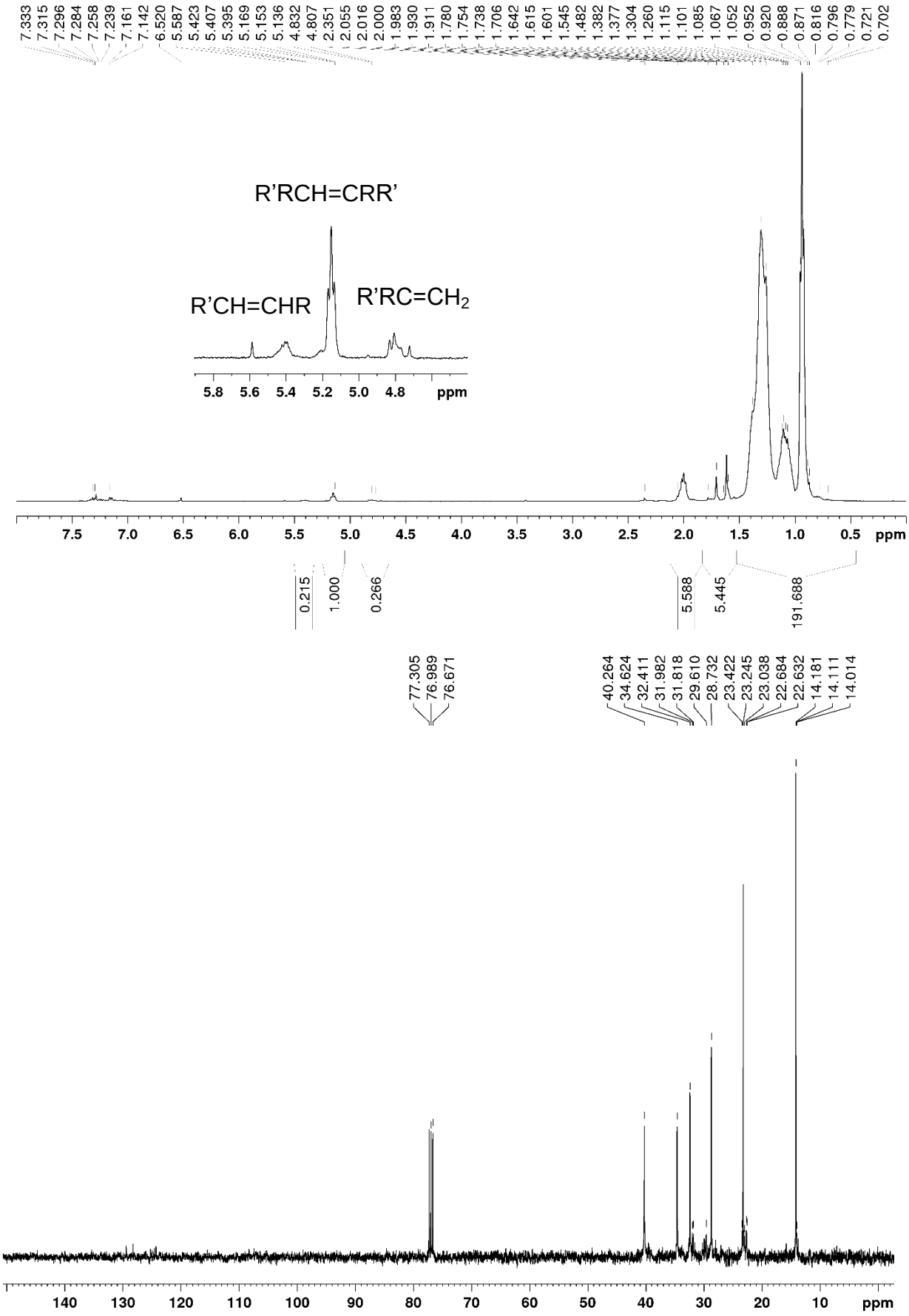

Figure S2. ^{1}H and ^{13}C NMR of 1-hexene oligomers obtained in the system *rac*-$H_4C_2[Ind]_2ZrCl_2$ (**1h**)- $HAlBu^{i}_2$-MMAO-12

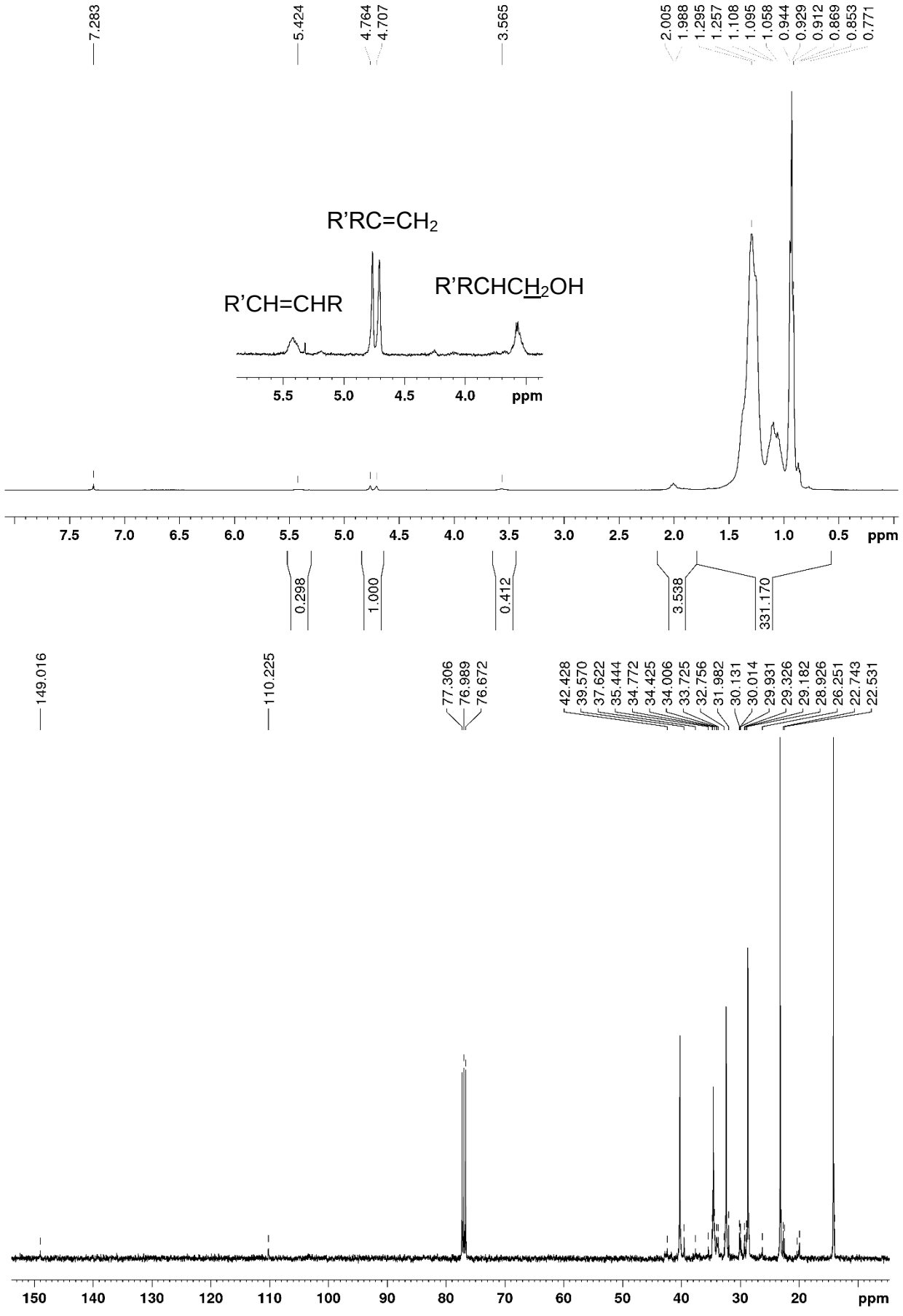

Figure S3. Comparison of ^{13}C NMR of 1-hexene oligomers obtained in the system Ind_2ZrCl_2 (**1f**)- $HAlBu^i_2$ activated by MMAO-12 and $(Ph_3C)[B(C_6F_5)_4]$.

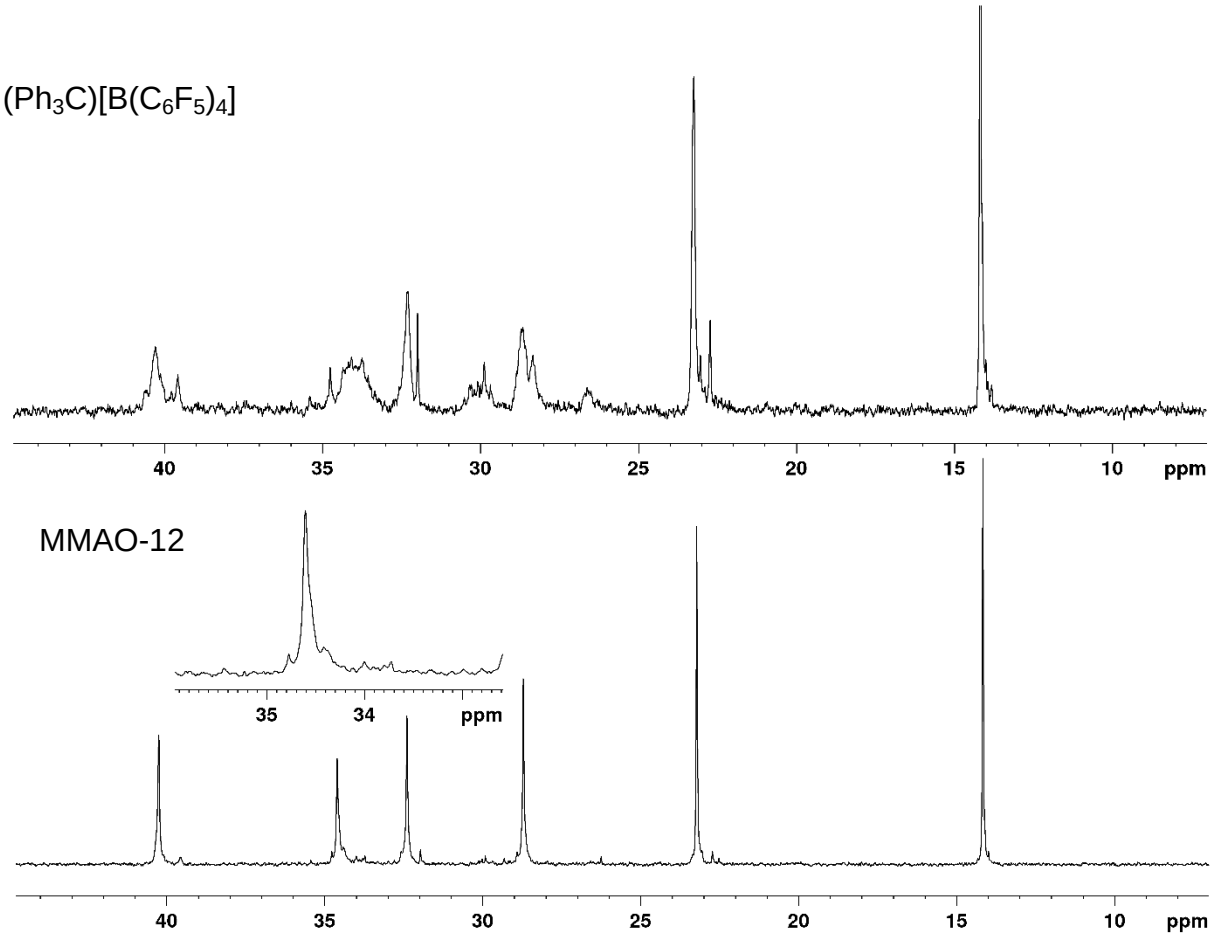

Figure S4. Comparison of ^{13}C NMR of 1-hexene oligomers obtained in the system *rac*-$Me_2CInd_2ZrCl_2$ (**1g**)- $HAlBu^i_2$ activated by MMAO-12 and $(Ph_3C)[B(C_6F_5)_4]$.

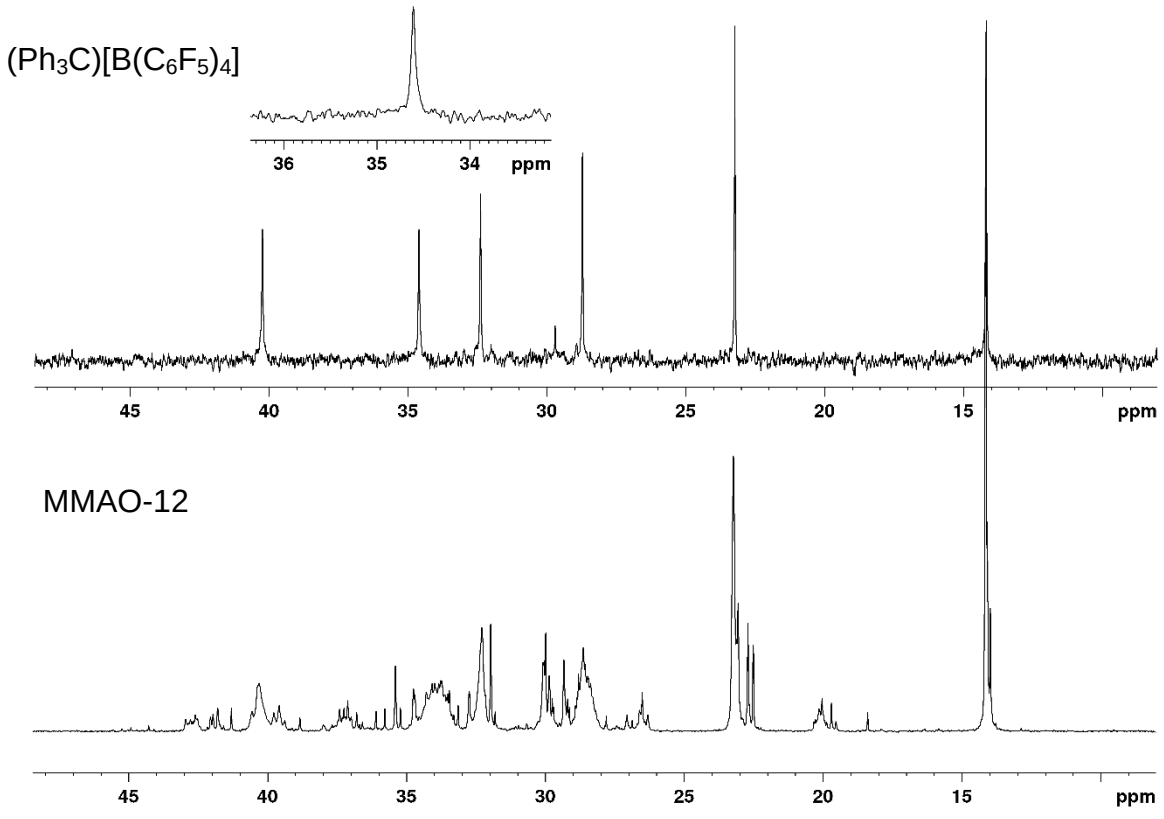

Figure S5. ^{1}H NMR of system $Me_2CCp_2ZrCl_2$ (**1c**) − $HAlBu^{i}_2$ (1:3) in C_7D_8 (250 K).

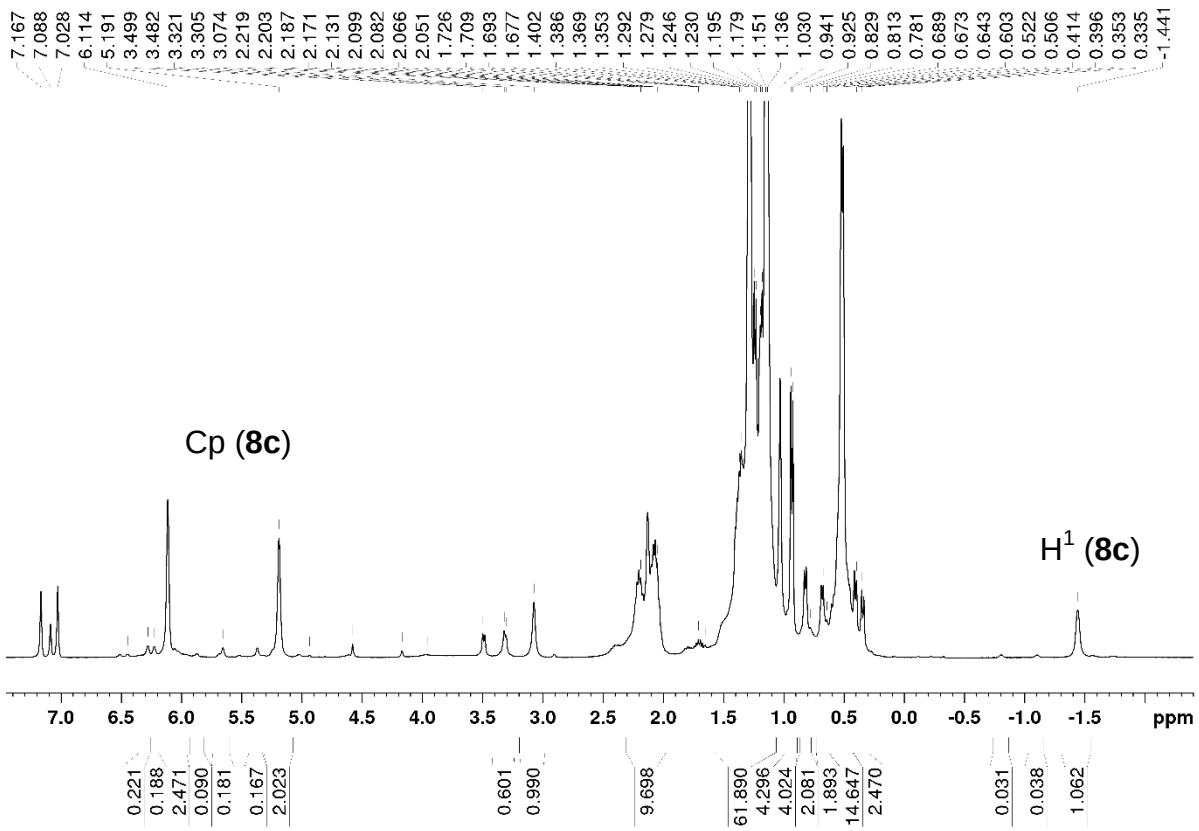

Figure S6. COSY HH of system $Me_2CCp_2ZrCl_2$ (**1c**) − $HAlBu^{i}_2$ (1:3) in C_7D_8 (250 K).

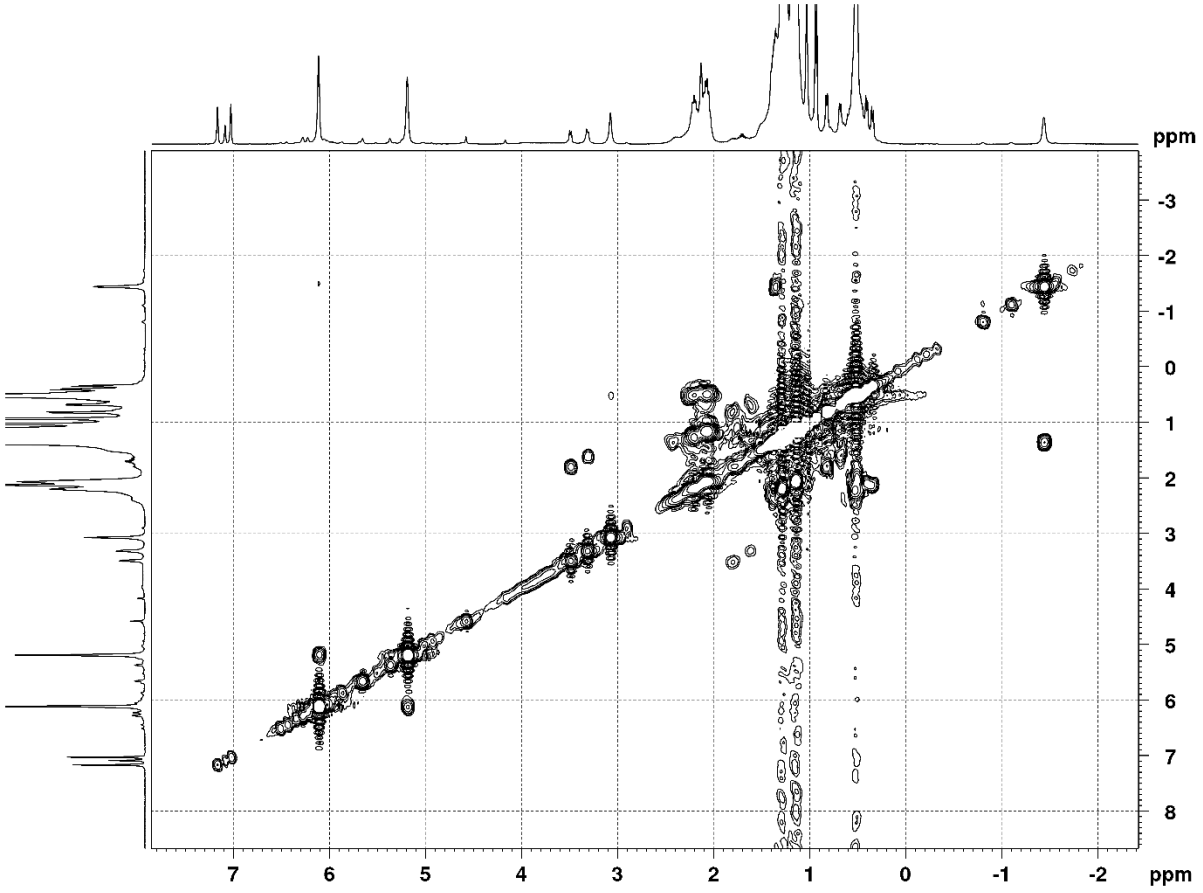

Figure S7. NOESY of system $Me_2CCp_2ZrCl_2$ (**1c**) − $HAlBu^i_2$ (1:3) in C_7D_8 (250 K).

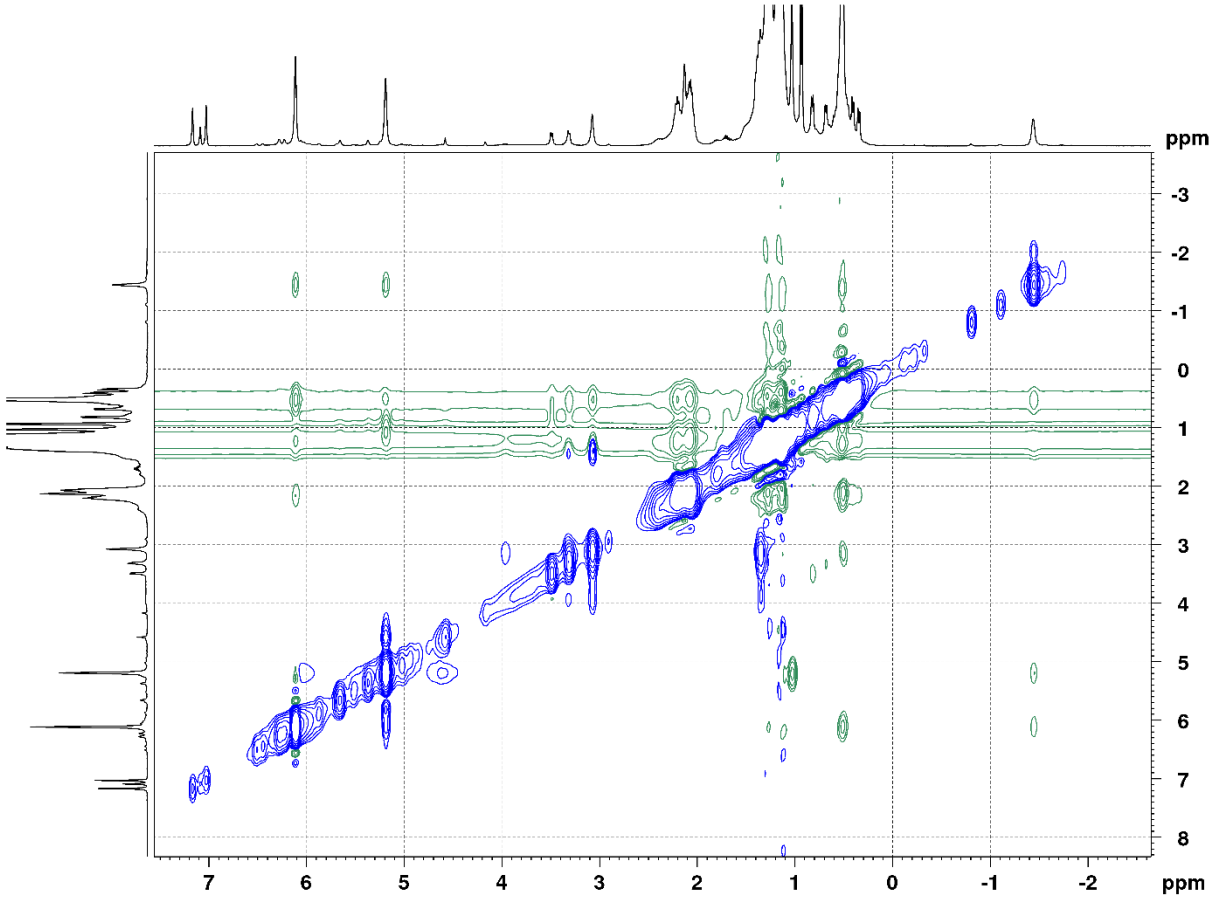

Figure S8. NOESY of system $Me_2CCp_2ZrCl_2$ (**1c**) − $HAlBu^i_3$ (1:8) in C_7D_8 (298 K).

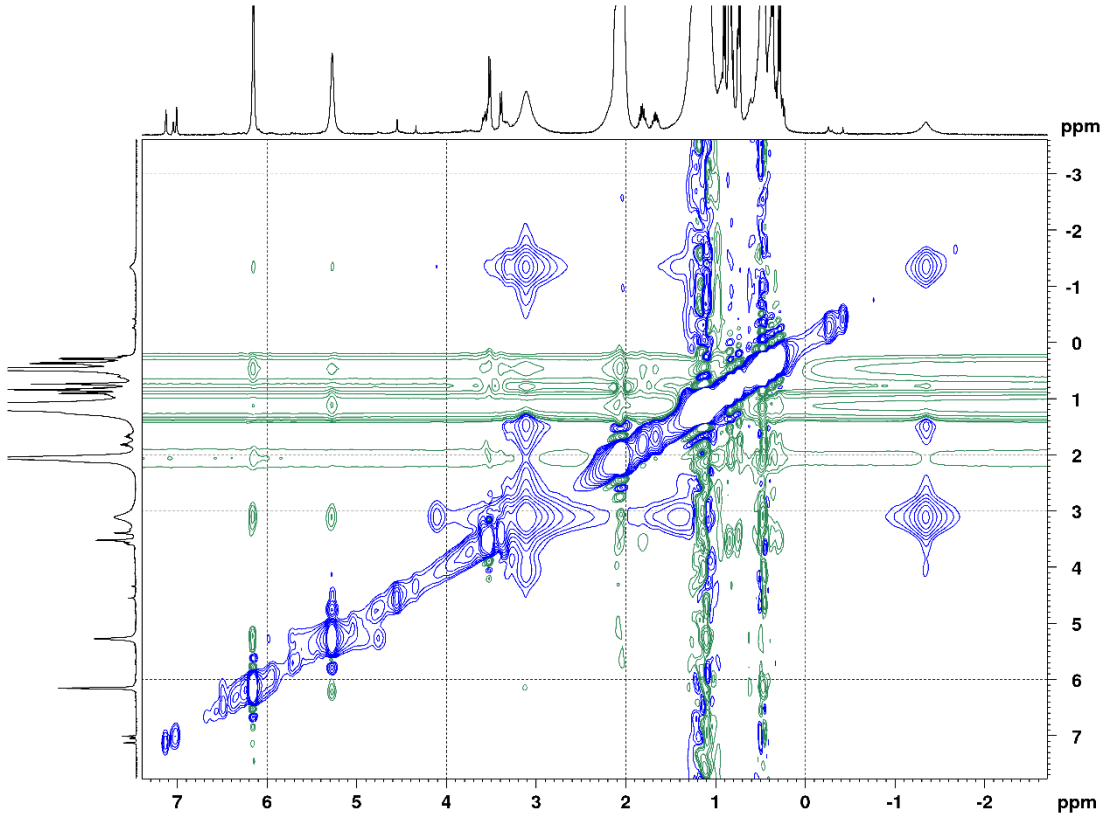

Figure S9. ^{1}H NMR of system $Me_2CCp_2ZrCl_2$ (**1c**) − $HAlBu^{i}_2$ (1:1.7) in C_7D_8 (298 K).

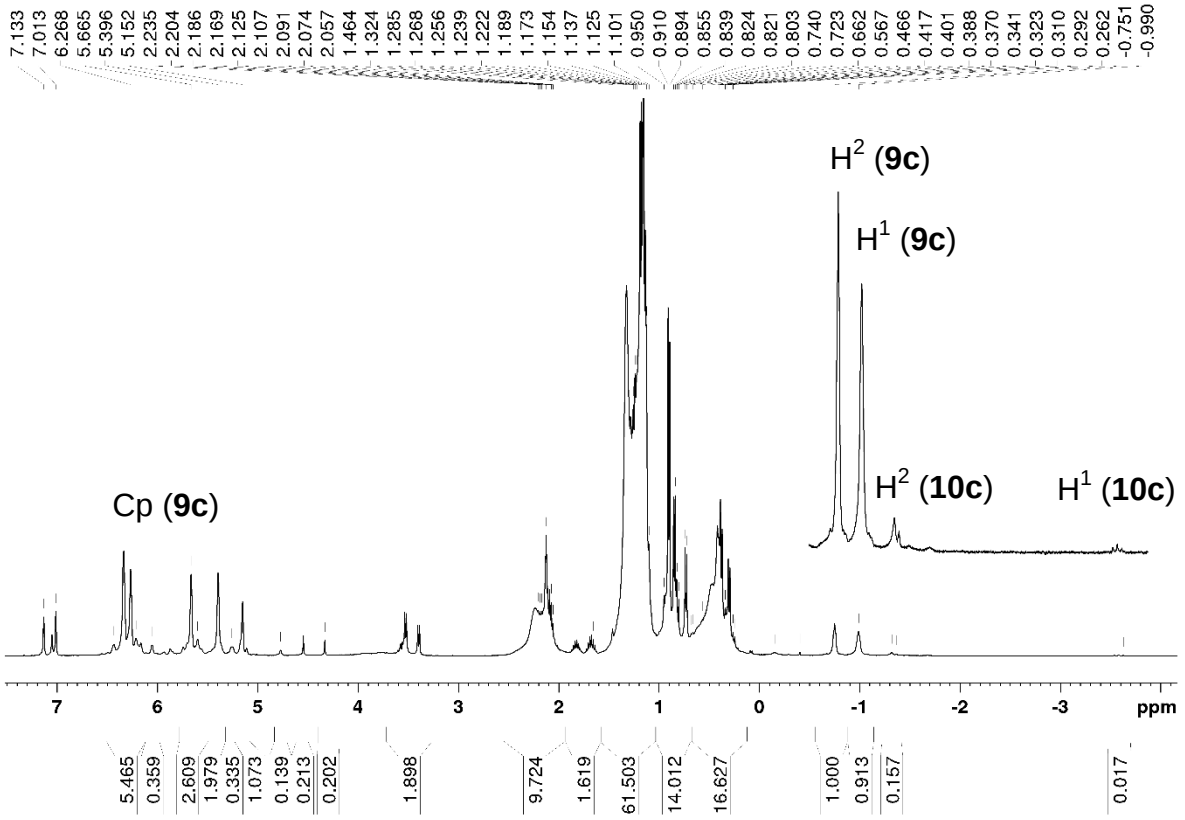

Figure S10. COSY HH of system $Me_2CCp_2ZrCl_2$ (**1c**) − $HAlBu^{i}_2$ (1:1.7) in C_7D_8 (298 K).

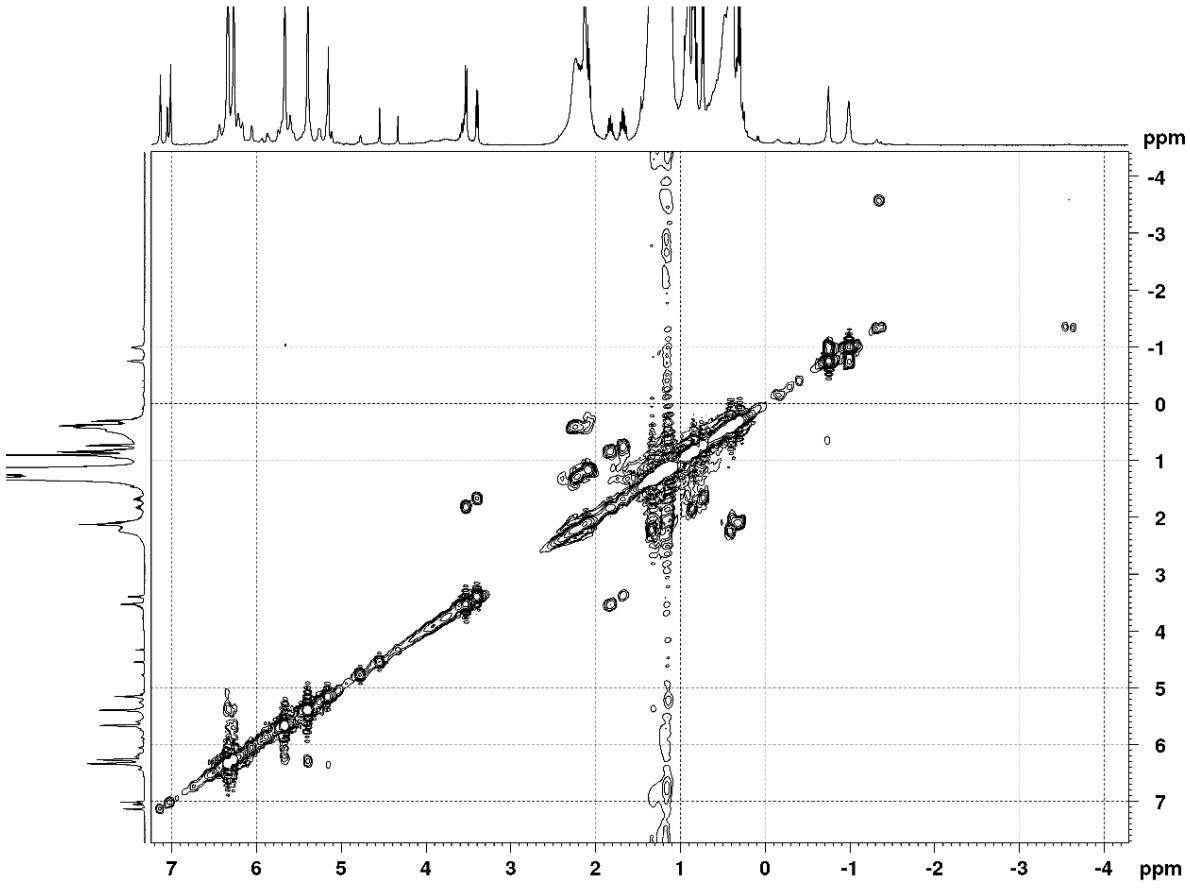

Figure S11. ^{1}H NMR of system MMAO-12 − $HAlBu^{i}_{2}$ (1:3) in C_7D_8 (298 K).

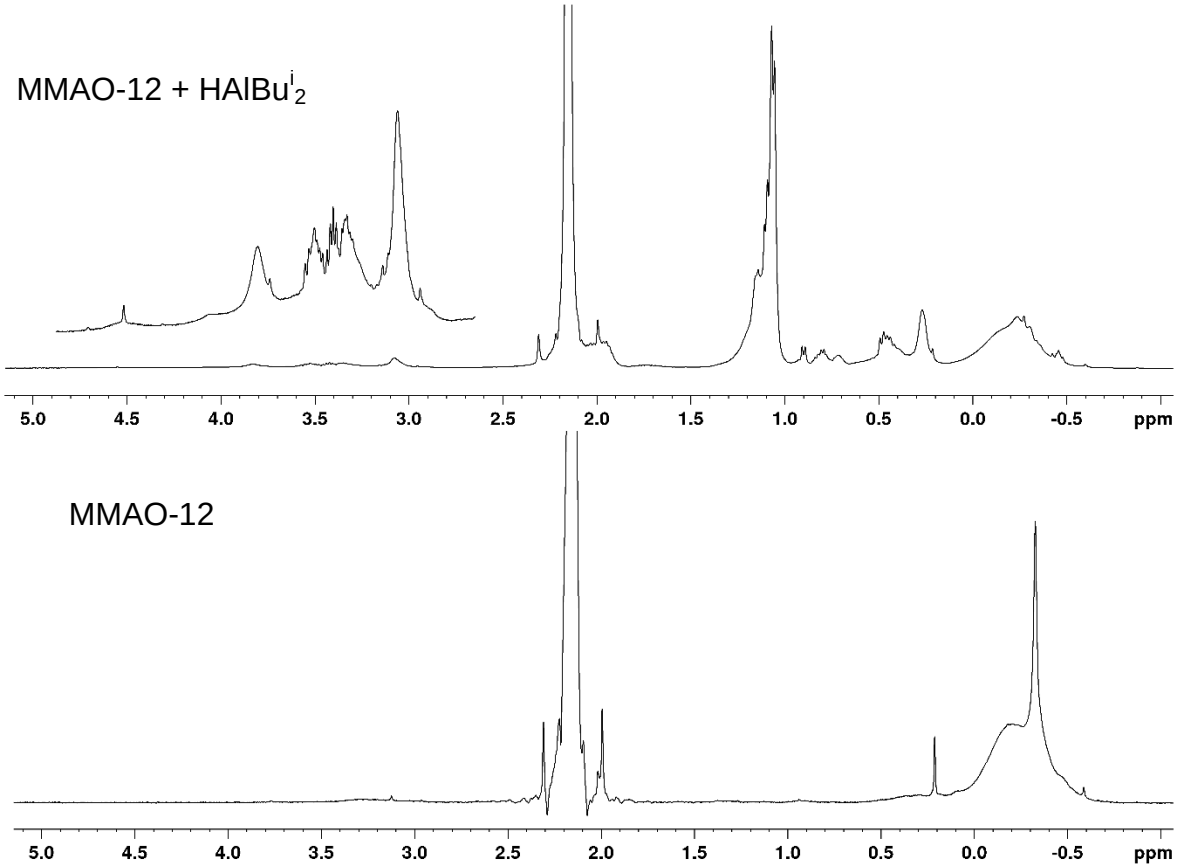

Figure S12. NOESY of system MMAO-12 − $HAlBu^{i}_{2}$ (1:3) in C_7D_8 (298 K).

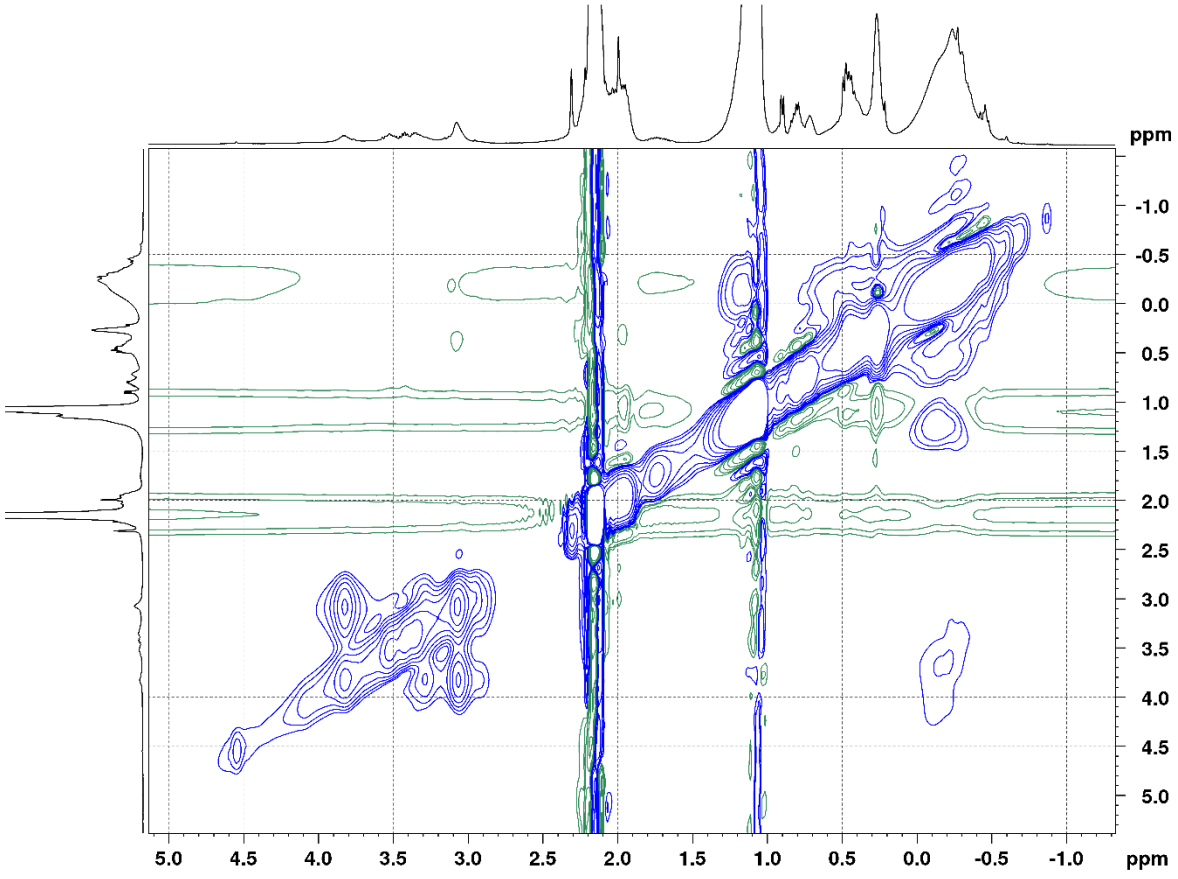

Figure S13. ^{1}H NMR of system $Me_2CCp_2ZrCl_2$ (**1c**) − $HAlBu^{i}_2$ − MMAO-12 (1:8:11) in C_7D_8 (298 K).

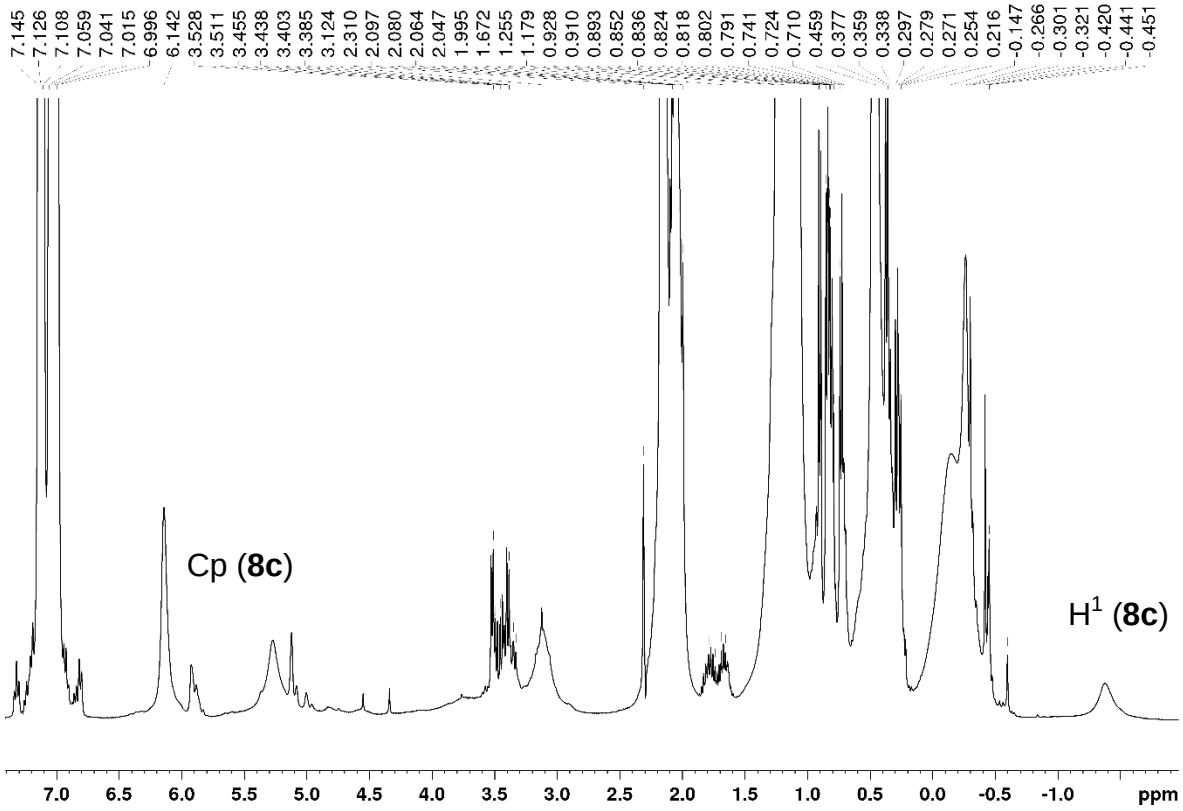

Figure S14. NOESY of system $Me_2CCp_2ZrCl_2$ (**1c**) − $HAlBu^{i}_2$ − MMAO-12 (1:8:11) in C_7D_8 (298 K).

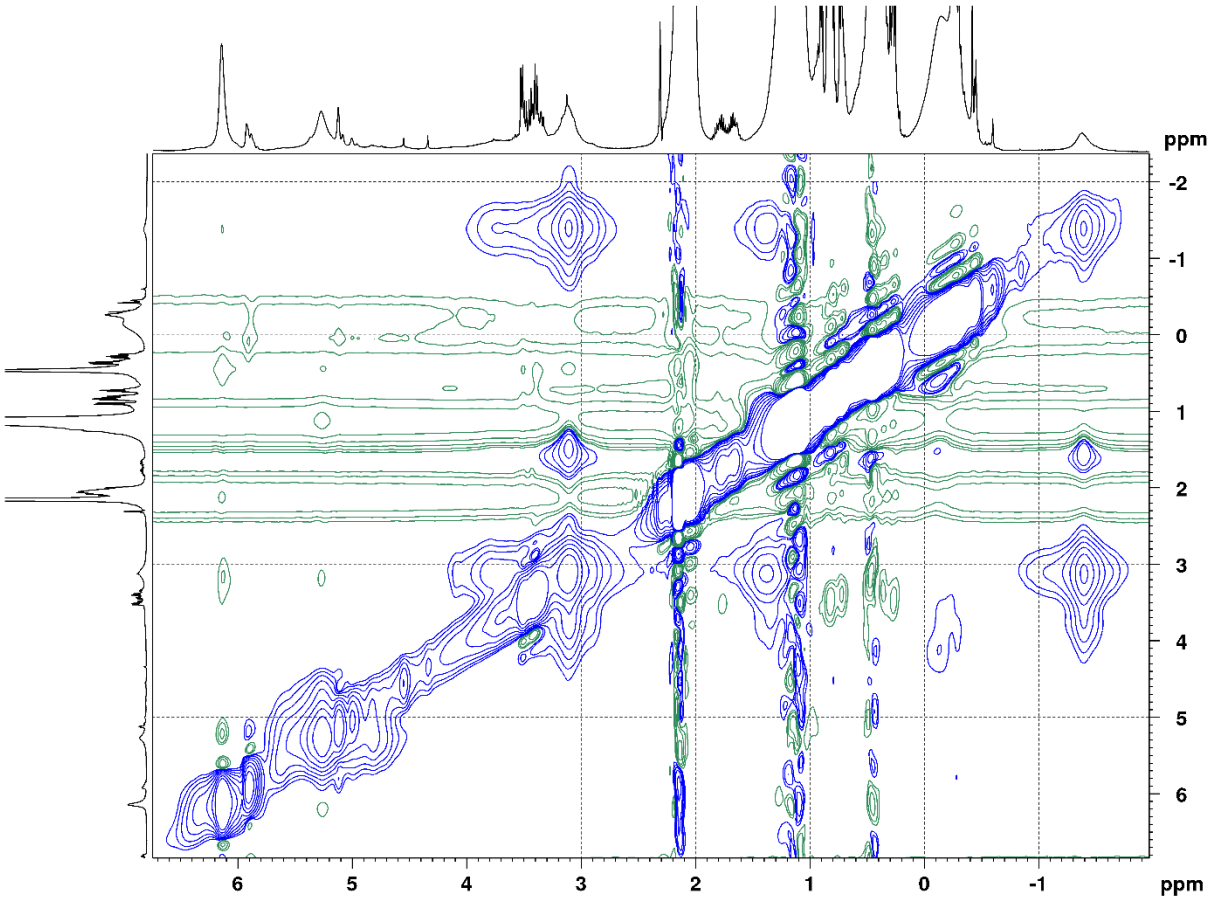

Figure S15. ^{1}H NMR of system $Me_2CCp_2ZrCl_2$ (**1c**) − $HAlBu^{i}_2$ – MMAO-12 (1:1.7:7) in C_7D_8 (298 K).

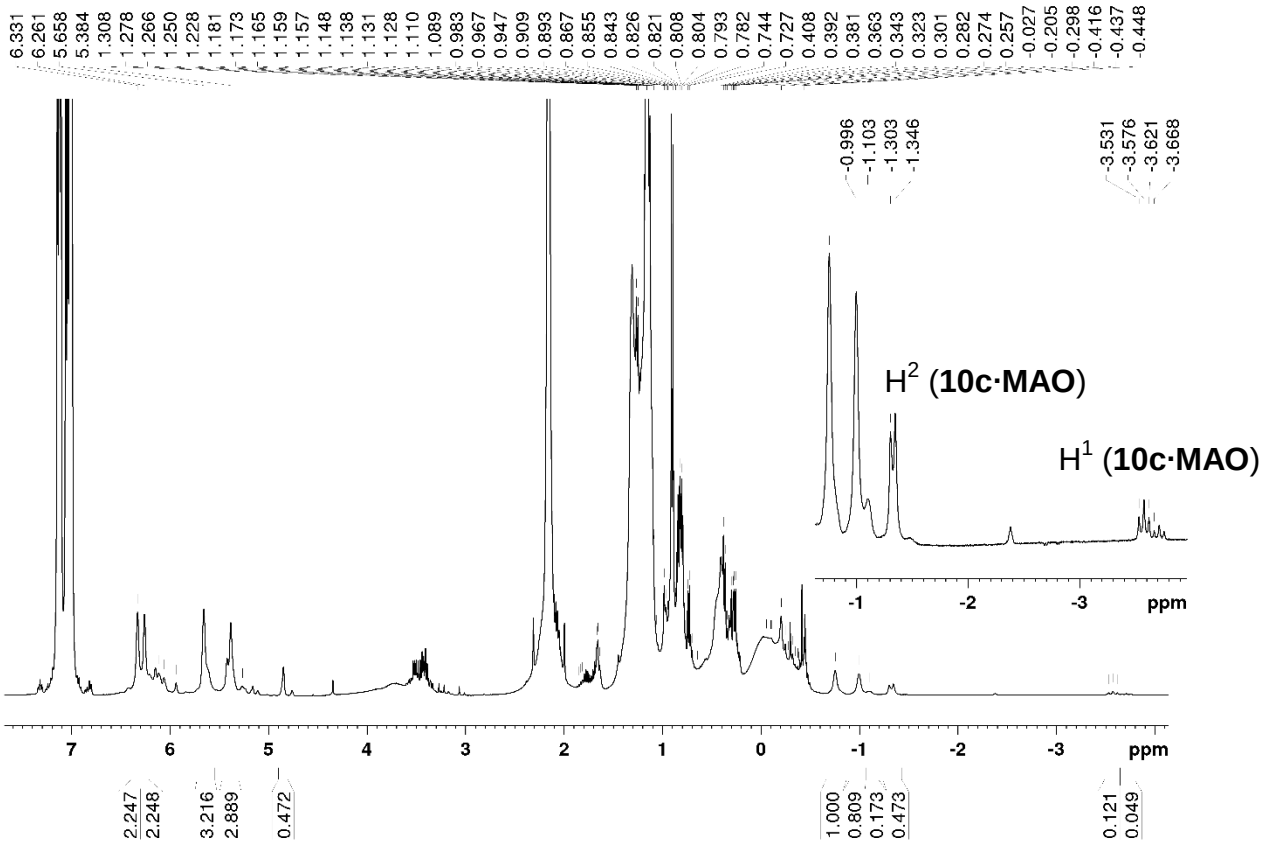

Figure S16. COSY HH of system $Me_2CCp_2ZrCl_2$ (**1c**) − $HAlBu^{i}_2$ – MMAO-12 (1:1.7:7) in C_7D_8 (298 K).

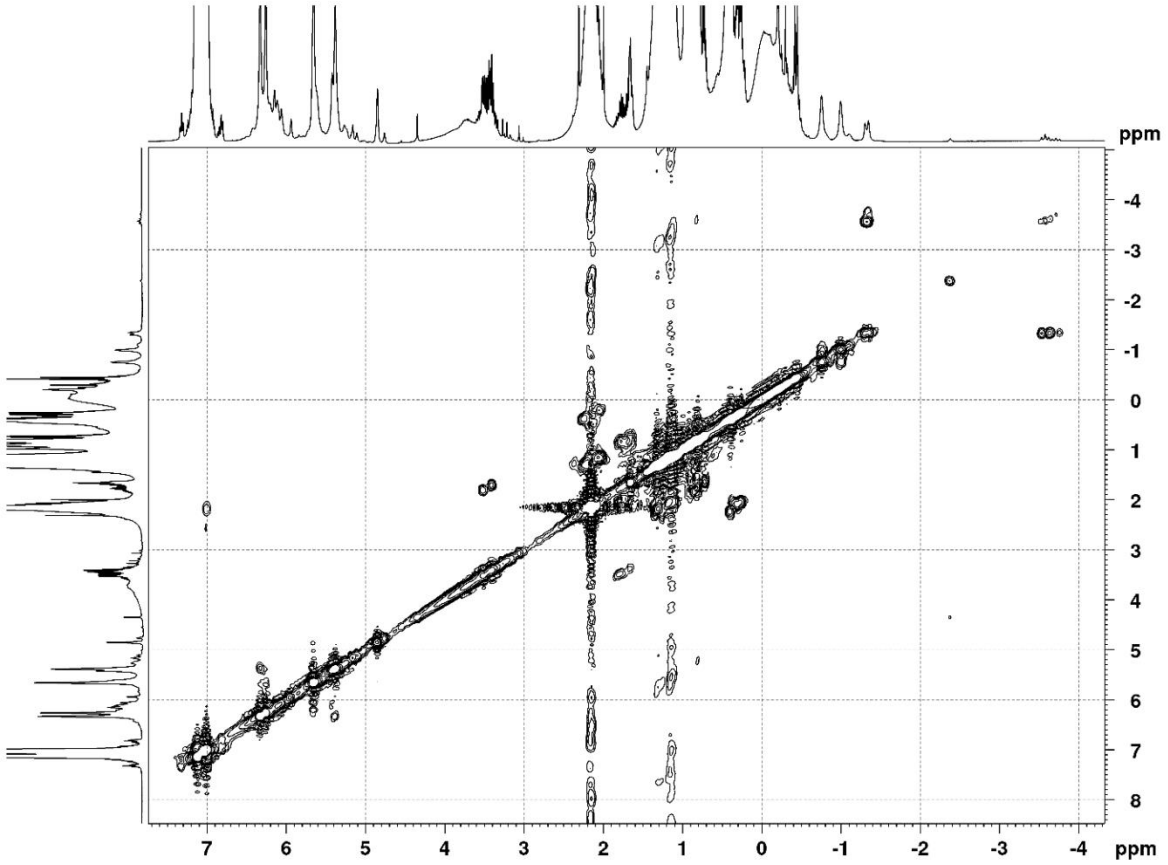

Figure S17. NOESY of system $Me_2CCp_2ZrCl_2$ (**1c**) − $HAlBu^i_2$ – MMAO-12 (1:1.7:7) in C_7D_8 (298 K).

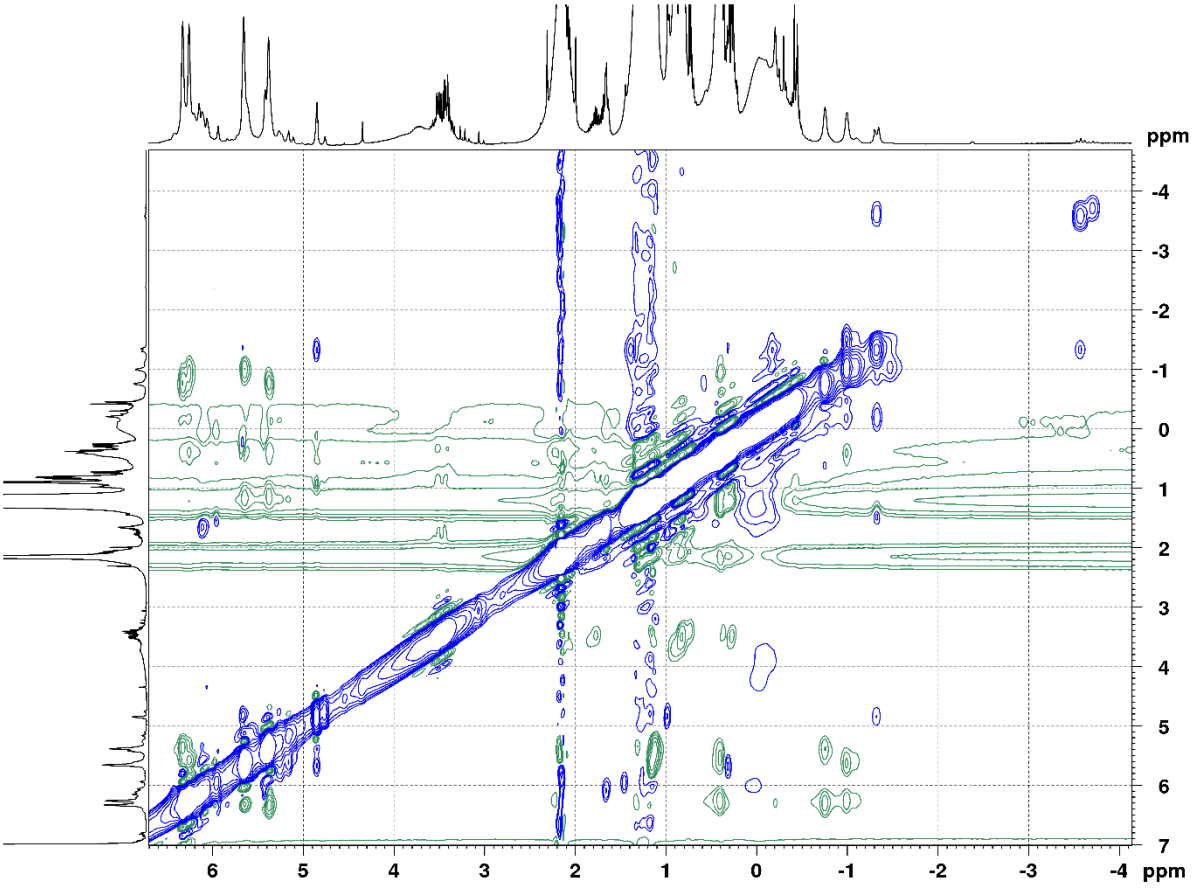

Figure S18. ^{1}H NMR of system $Me_2CCp_2ZrCl_2$ (**1c**) − $HAlBu^{i}_2$ – $(Ph_3C)[B(C_6F_5)_4]$ (1:1:0.1) in C_7D_8 (298 K).

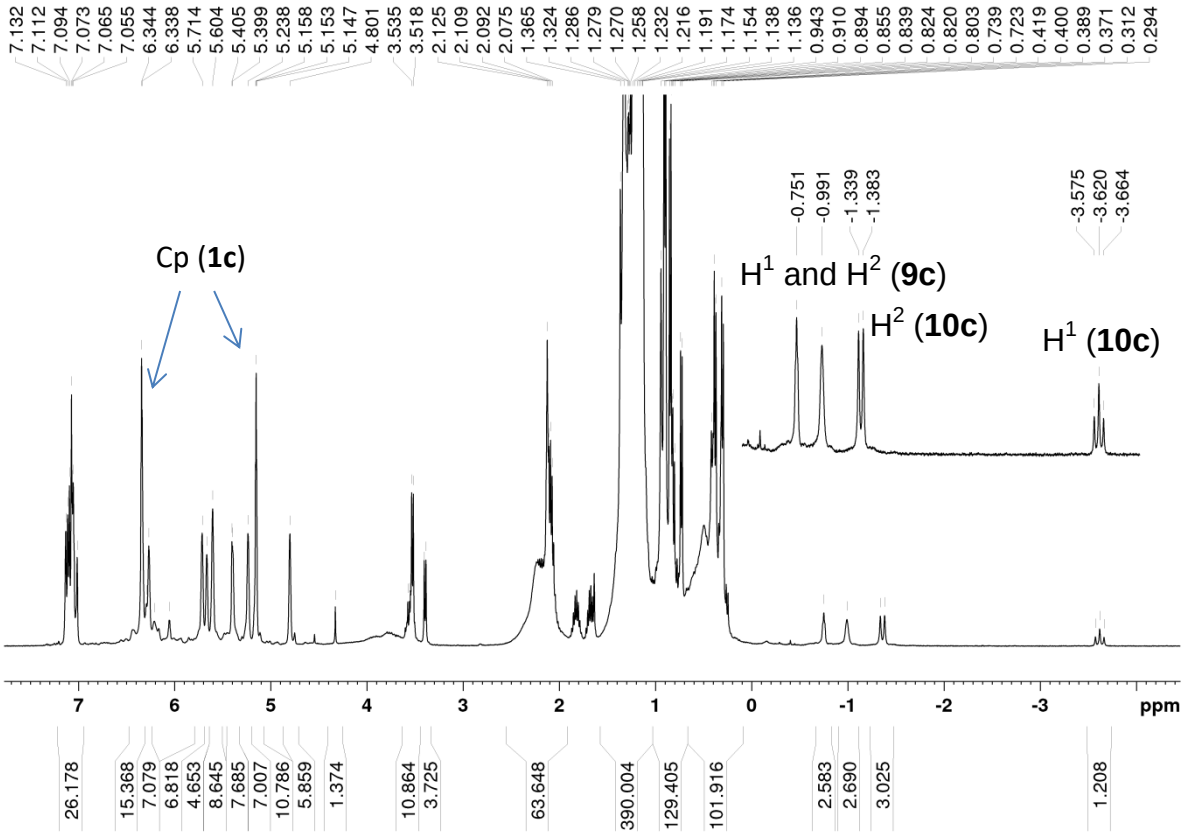

Figure S19. COSY HH of system $Me_2CCp_2ZrCl_2$ (**1c**) − $HAlBu^{i}_2$ – $(Ph_3C)[B(C_6F_5)_4]$ (1:1:0.1) in C_7D_8 (298 K).

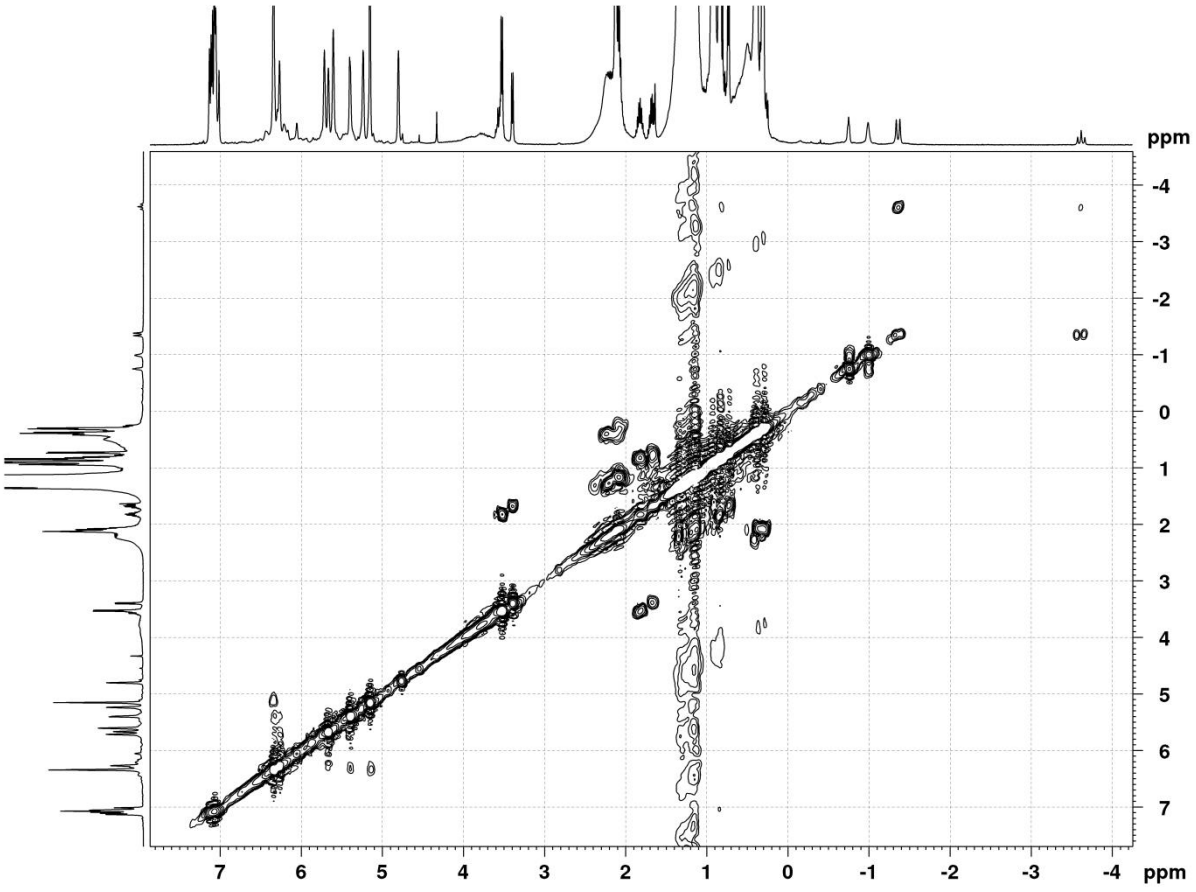

Figure S20. NMR monitoring of system $Me_2CCp_2ZrCl_2$ (**1c**) − $HAlBu^i_2$ − MMAO-12 – 1-hexene (1:8:11:2) in C_7D_8.